Applied Surface Science 258 (2011) 408–413

Contents lists available at SciVerse ScienceDirect

Applied Surface Science

journal homepage: www.elsevier.com/locate/apsusc

Adsorption and dissociation of O_2 on CuCl(1 1 1) surface: A density functional theory study

Riguang Zhang, Hongyan Liu, Baojun Wang*, Jun Ren, Zhong Li

Key Laboratory of Coal Science and Technology of Ministry of Education and Shanxi Province, Taiyuan University of Technology, No. 79 Yingze West Street, Taiyuan 030024, Shanxi, China

ARTICLE INFO

Article history:
Received 26 June 2011
Received in revised form 30 August 2011
Accepted 30 August 2011
Available online 7 September 2011

Keywords:
Oxygen
CuCl(1 1 1)
Adsorption
Dissociation
Density functional theory

ABSTRACT

The adsorption and dissociation of O_2 on CuCl(1 1 1) surface have been systematically studied by the density functional theory (DFT) slab calculations. Different kinds of possible modes of atomic O and molecular O_2 adsorbed on CuCl(1 1 1) surface and possible dissociation pathways are identified, and the optimized geometry, adsorption energy, vibrational frequency and Mulliken charge are obtained. The calculated results show that the favorable adsorption occurs at hollow site for O atom, and molecular O_2 lying flatly on the surface with one O atom binding with top Cu atom is the most stable adsorption configuration. The O–O stretching vibrational frequencies are significantly red-shifted, and the charges transferred from CuCl to oxygen. Upon O_2 adsorption, the oxygen species adsorbed on CuCl(1 1 1) surface mainly shows the characteristic of the superoxo (O_2^-), which primarily contributes to improving the catalytic activity of CuCl, meanwhile, a small quantity of O_2 dissociation into atomic O also occur, which need to overcome very large activation barrier. Our results can provide some microscopic information for the catalytic mechanism of DMC synthesis over CuCl catalyst from oxidative carbonylation of methanol.

1. Introduction

Dimethyl carbonate (DMC) has drawn continuous attention from researchers due to its applications in replacing environmentally unfriendly compounds, in which the direct oxidative carbonylation of methanol with CO and O_2 in liquid phase using CuCl as catalyst is one of important commercial processes for the production of DMC [1]. In the last two decades, new catalysts were developed to solve the problem in terms of catalyst deactivation and vessel corrosion [2]. High catalytic activity and selectivity have been obtained on homogeneous catalytic systems by properly choosing the supporting ligand [3–6]. Meanwhile, attempts were made to heterogenized homogenous catalyst systems by immobilizing CuCl or $CuCl_2$ on polymer supports [7,8] or mesoporous materials [9]. In addition, the development of low chlorine content or chloride-free catalyst systems for DMC synthesis is also a suggested new direction [10–12].

All along, the main researches of our group focus on DMC synthesis from direct oxidative carbonylation of methanol with CO and O_2 in liquid phase using CuCl as catalyst [13–19], for example, our recent experiments [14–16] have obtained the CuCl/SiO_2–TiO_2 catalyst of CuCl supported on the silica–titania (SiO_2–TiO_2) materials, and DMC could be synthesized on CuCl/SiO_2–TiO_2 catalyst. Further, CuCl/SiO_2–TiO_2 catalyst shows better catalytic performance and reduced corrosion, in which CuCl is the catalytic active species. Besides, CuCl(1 1 1) polar surface is an ideal unrelaxed surface [20,21], and the coordinated unsaturated Cu(I) sites on CuCl(1 1 1) surface have been proposed as the active centers for the high activity catalysts [22].

Several studies about the mechanism of DMC synthesis over Cu-based catalysts from direct oxidative carbonylation of methanol have shown that CH_3O adsorbed on catalyst surface is an important intermediate in reaction, in which the presence of oxygen species on catalyst surface plays a pivotal role for the formation of CH_3O. For example, based on evidence from in situ IR spectroscopy, King [23,10] has proposed that CH_3OH adsorbs on extra-framework Cu cations in Cu–Y and quickly reacts with oxygen species to form CH_3O, then, CO addition to adsorbed CH_3O produces carbomethoxide species. Meanwhile, the studies by Anderson et al. [24,25] and Zhang and Bell [26] have shown that CH_3O adsorbed on Cu-based catalyst can be easily formed by CH_3OH decomposition in the presence of oxygen species. Further, Chen et al. [27] found that the surface oxygen exhibited a high surface reactivity towards the formation of CH_3O by CH_3OH decomposition on CuCl surface, which means that the interaction of oxygen species with CuCl surface is an important component of the catalytic activity of CuCl in DMC synthesis. But it is not clearly understood about the detailed interaction of oxygen species with CuCl catalyst involving in the adsorption

* Corresponding author. Tel.: +86 351 6018539; fax: +86 351 6041237.
E-mail addresses: wangbaojun@tyut.edu.cn, quantumtyut@126.com (B. Wang).

0169-4332/$ – see front matter © 2011 Elsevier B.V. All rights reserved.
doi:10.1016/j.apsusc.2011.08.130

site, charge transfer, especially, the existent state of oxygen species on the surface and the catalytic process.

Over the past decades, it has been demonstrated that theoretical techniques can serve as powerful tools for providing qualitative and quantitative insights into the structure of active surface and surface interaction [28–31]. To our knowledge, few theoretical studies about the interaction of oxygen species with CuCl have been systematically reported, which will be helpful to deeply probe into the existent state of oxygen species on CuCl surface, as well as the catalytic activity of CuCl at a microscopic level. Nowadays, only Wang et al. [32] investigated the adsorption behavior of oxygen species on CuCl(1 1 1) surface by using denstity functional theory (DFT) method, however, the catalytic process of molecular oxygen dissociation has not been mentioned. In fact, the dissociation process of molecular oxygen on CuCl surface is an important component of the interaction of oxygen species with CuCl to probe into the existent state of oxygen species and the catalytic activity of CuCl.

Therefore, in this study, DFT calculations are performed to investigate the adsorption of molecular oxygen and its dissociation product, atomic oxygen, on CuCl(1 1 1) surface, to elucidate the existent state of oxygen species and corresponding origin, as well as to understand the active centers presented on CuCl(1 1 1) surface and the microscopic mechanism behind the reaction that occur on CuCl(1 1 1) surface, which may be of interest to researchers attempting to illustrate the catalytic mechanism for DMC formation from oxidative carbonylation of methanol. The major issue that we address is determination of the preferred adsorption site and stable configuration of atomic and molecular oxygen on CuCl(1 1 1) surface, as well as the dissociation process of O_2 on CuCl(1 1 1) surface.

2. Computational models and methods

2.1. Surface models

Based on the structure of bulk CuCl, CuCl(1 1 1) surface is modeled to study the adsorption properties by using the supercell approach, where periodic boundary condition are applied to the central supercell so that it is reproduced periodically throughout space. The CuCl(1 1 1)-[2 × 2] supercell model including six atomic layers and the corresponding four different adsorption sites (top, bridge, hollow and Cl-site) are employed, as shown in Fig. 1 (the side and top view of CuCl(1 1 1) surface). A vacuum layer of 10 Å along the *z*-direction perpendicular to the surface (*x* and *y* being parallel) is employed to prevent spurious interactions between the repeated slabs. No relaxation or reconstruction has been observed according to the experimental results by LEED methods and theoretical results [20,21,33–35]. Meanwhile, previous studies by our group [13] and Chen et al. [27,36–38] about the adsorption and dissociation of small molecules such as O_2, CO on CuCl(1 1 1) surface have also suggested that the relaxation of CuCl(1 1 1) surface is negligible and could been frozen in the calculation. Therefore, the adsorbed atomic O and molecular O_2 are allowed to relax in all of the geometry optimization calculations and the substrate is kept fixed to the bulk coordinates.

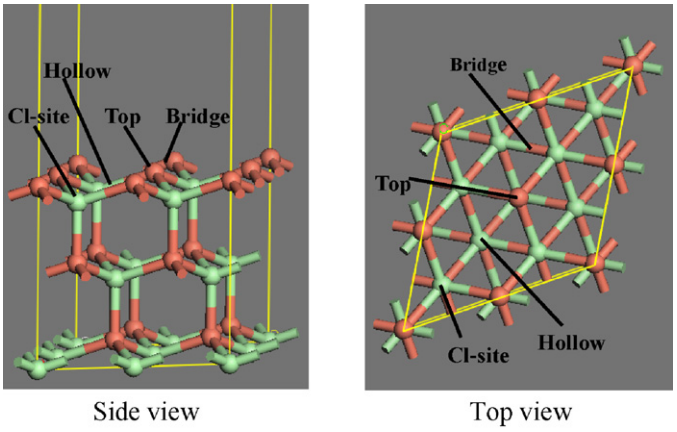

Fig. 1. The slab model of CuCl(1 1 1)-(2 × 2) supercell (top view and side view). Green balls represent Cl atoms, orange balls represent Cu atoms. (For interpretation of the references to color in this figure legend, the reader is referred to the web version of the article.)

2.2. Calculation methods

In our study, DFT has been employed to perform for all calculations. The exchange-correlation functional of generalized gradient approximations (GGA) is used, which can give very much better results for the adsorption energies [39,40] and dissociation energies [41,42]. The main calculations presented here are based on the GGA of Perdew and Wang (PW91) [43,44]. The valence electron functions are expanded into a set of numerical atomic orbitals by a double-numerical basis with polarization functions (DNP) [45]. Brillouin-zone integrations have been performed using 3 × 3 × 1 Monkhorst-Pack grid. The inner electrons of copper atoms are kept frozen and replaced by an effective core potential (ECP) [46,47], and oxygen and chlorine atoms are treated with an all-electron basis set. All calculations are carried out with the Dmol^3 program package in Materials Studio 4.4 [48,49].

In order to evaluate the reliability of the calculation methods, we calculate the bond length and stretching frequency of molecular O_2 by our approach, the calculated results are r(O–O) = 0.122 nm and ν_{C-O} = 1557 cm^{-1}, which agree with the experimental values of 0.121 nm [50] and 1555 cm^{-1} [51], as well as to other similar GGA results [32,52,53]. Then, the test is to predict the lattice constant of bulk CuCl, the calculated value for the lattice constant of CuCl (0.5521 nm) is close to the experimental equilibrium lattice constant of 0.5406 nm [54]. These results obtained in above tests make us confident in the reliability of our calculation methods.

3. Results and discussion

The adsorption energy (E_{ads}) is always regarded as a measure of the strength of adsorbate–substrate adsorption. E_{ads} is defined as follows:

$$E_{ads} = E_{sub} + E_{mol} - E_{mol/sub}$$

where $E_{mol/sub}$ is the total energy of adsorbate–substrate system in the equilibrium state, E_{sub} and E_{mol} are the total energies of substrate and free adsorbate alone, respectively. With this definition, more positive values reflect strong interaction of adsorbed species with surface atoms. In this study, for the adsorption of atomic or molecular oxygen, the true (triplet) ground state is entered into this definition, irrespective of whether the adsorbed system is in the single or triplet state.

3.1. Atomic oxygen adsorption on CuCl(1 1 1) surface

The adsorption of atomic O on CuCl(1 1 1) surface is calculated at a coverage of 0.25 monolayer (ML) with one atomic oxygen in every (2 × 2) unit cell. Four distinct adsorption sites presented in Fig. 1 are examined. The values of the calculated adsorption energies, the optimized geometries and Mulliken charges for atomic O adsorbed on the surface are listed in Table 1.

In the case of atomic O adsorption at bridge site and Cl-site, it is found that the initial configurations of bridge and Cl-site are converted to hollow configuration after optimization. O adsorbed

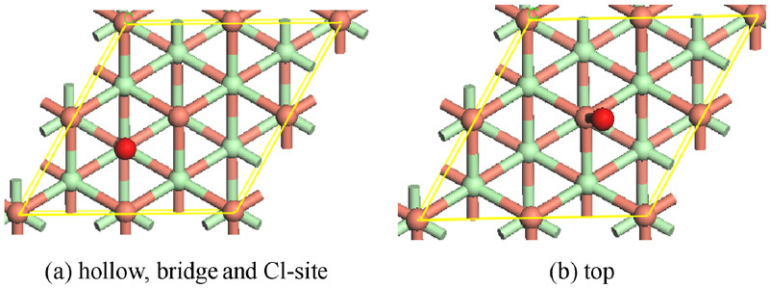

Fig. 2. The optimized configuration of atomic O coordinated at different adsorption sites. Red ball stands for O atom, and others are the same as in Fig. 1. (For interpretation of the references to color in this figure legend, the reader is referred to the web version of the article.)

Table 1
The calculated properties for atomic oxygen adsorbed on CuCl(1 1 1) surface.

Adsorption sites	d(O–Cu)/nm	q(O)	E_{ads}/kJ mol^{-1}
Top	0.179	−0.535	305.0
Hollow	0.237	−0.553	310.0

at hollow site has the largest adsorption energy of 310.0 kJ mol^{-1}. Meanwhile, the optimized configuration of O adsorbed at top site still bounds to top site with the adsorption energy of 305.0 kJ mol^{-1}. In addition, the Mulliken charges also support the results from the adsorption energy; we can see that the electron transfers from substrate to adsorbate as the atomic oxygen binds to copper, and the net charge of atomic oxygen for hollow and top configurations are 0.553 *e* and 0.535 *e*, respectively. Hence, above results indicate that hollow and top sites are the active centers for atomic O adsorbed on CuCl(1 1 1) surface, and hollow site is the preferred site, which agrees with the previous work by Wang et al. [32]. The optimized geometrical structures of atomic O adsorbed at hollow and top sites are shown in Fig. 2.

Based on the adsorption of atomic O, we suspect that there may be two products for the dissociation of O_2 into atomic O on CuCl(1 1 1) surface. One is called P1, i.e., two atomic O are adsorbed at two adjacent hollow sites, as shown in Fig. 3(a), the other is called P2, i.e., one atomic O is adsorbed at hollow site and the other bounds to the close top site, as presented in Fig. 3(b). However, the calculated results show that the initial co-adsorption structure of two atomic O adsorbed at hollow site and the close top site (P2) is optimized to the co-adsorption configuration of two atomic O adsorbed at the adjacent two hollow sites (P1) after optimization. The optimized structures of P1 and P2 are presented in Fig. 3(c).

3.2. O_2 adsorption on CuCl(1 1 1) surface

Since the triplet state is the ground stated of the free O_2 molecule [53,55], the adsorption of O_2 in the triplet state on CuCl(1 1 1) surface is systematically investigated at a coverage of 1/4 ML with one molecule in every (2×2) unit cell. However, for completeness we also calculated a few results for O_2 adsorption in the singlet state. Two adsorption types of O_2 at four distinct sites (see Fig. 1) have been considered: one is an end-on type involving O_2 vertical to the surface, the other is a side-on type involving O_2 parallel to the surface, and the corresponding geometries used in the calculations are depicted in Fig. 4. The calculated adsorption properties are listed in Table 2, and the optimized equilibrium configurations of O_2 are presented in Fig. 5.

According to Table 2, we can also see that in the case of the triplet state, for the end-on type, it is interesting to find that the initial configuration of top-V is converted to M1 mode after optimization, as shown in Fig. 5(a). Bridge-V and Cl site-V configurations are converted to M2 mode (see Fig. 5(b)), and hollow-V configuration is converted to M3 mode (see Fig. 5(c)). For the side-on mode, in the case of top-P, Cl site-P and hollow-P configurations, they are converted to M2 mode. Bridge-P configuration is converted to M1 mode. In the case of singlet state, only the adsorption of hollow-V configuration is converted to M3 mode, other configurations are all converted to M2 mode. Moreover, there are only small differences in adsorption energies and adsorption geometry between singlet and triplet electronic states. The adsorption energy in the triplet state is slightly larger than that in the singlet state, whereas the O–O distance in the triplet state is slightly shorter than that in the singlet state. Therefore, we will only discuss the adsorption of O_2 in the triplet state on CuCl(1 1 1) surface below, since the triplet state is the ground stated of the free O_2 molecule.

In M1 mode, the adsorbed O_2 lies flatly over singly coordinate Cu–Cu bridge on CuCl(1 1 1) surface, the corresponding O–O bond length of adsorbed O_2 is elongated to 0.133 nm from 0.122 nm in free O_2 molecule, which has an adsorption energy of 138.9 kJ mol^{-1}. The Mulliken charges show that electron transfer from substrate to O_2 is 0.400 *e*. In M2 mode, O_2 lies flatly on the surface with one O atom binding with the top Cu atom, and the O–O bond length of O_2 is elongated to 0.135 nm, which is the most stable adsorption configuration with the largest adsorption energy of 146.1 kJ mol^{-1}. The electron transfer from substrate to O_2 is 0.440 *e*. For M3 mode, it has an adsorption energy of 87.9 kJ mol^{-1} with O_2 vertically adsorbed at hollow site, in which the O–O bond length is 0.131 nm, and the electron transfer from substrate to O_2 is 0.375 *e*. From M1 to M3 modes, we can see that O_2 adsorbed on CuCl(1 1 1) surface is neg-

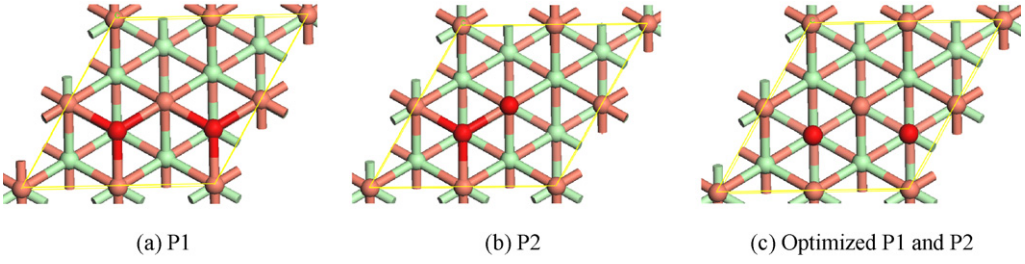

Fig. 3. The initial structures of P1 and P2, as well as the optimized structures of P1 and P2. See Figs. 1 and 2 for color coding.

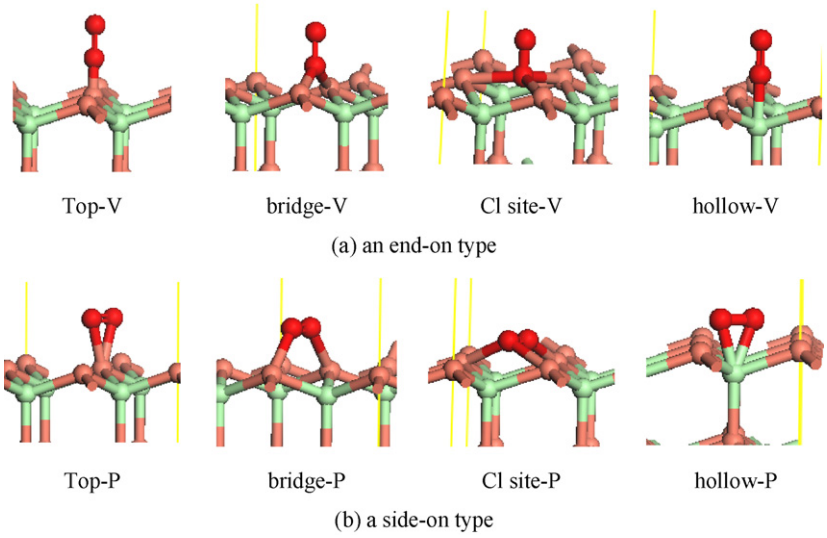

Fig. 4. The adsorption geometrical types of O_2 at different sites on CuCl(1 1 1) surface. See Figs. 1 and 2 for color coding.

atively charged, and the O–O bond length is longer than that of free O_2. Thus, the more negative the charges of the adsorbed O_2 are, the longer the O–O bond length is, and the more strongly the intramolecular O–O bond is activated by adsorption.

Vibrational spectroscopy has shown the existence of a peroxo form (O_2^{2-}), with a stretching frequency of ~766 cm^{-1}, and a superoxo (O_2^-) form, with a stretching frequency of ~1097 cm^{-1}. As shown in Table 2, the $\nu(O_2)$ scatters over a wide range from 919 to 1151 cm^{-1}, the O–O bond length of adsorbed O_2 (0.131–0.136 nm) is close to that of the O_2^- ion (0.128 nm). All of these suggest that upon O_2 adsorption, the oxygen species adsorbed on CuCl(1 1 1) surface is assigned to the characteristic of the superoxo (O_2^-). Although there are no experimental data available for comparison with our calculated results, the calculated vibrational frequencies can serve as good indicators for future experiments in this area. Meanwhile, it is observed that the O–O stretching frequency of the adsorbed O_2 on CuCl(1 1 1) surface is red-shift, which agrees with the experimental results by Zhang et al. [57]. The trend of vibrational frequency agrees with that of bond length and Mulliken charges of the adsorbed O_2. In other words, significant charge transfer from the substrate to oxygen species can weaken the intensity of the O–O bond, causing it to lengthen and reducing its frequency.

Therefore, in the view of the O–O bond lengths and adsorption energies, M1–M3 modes are the stable adsorption configurations towards the dissociation of O_2. M2 mode, O_2 lying flatly on the surface with one O atom binding with top Cu atom on CuCl(1 1 1) surface, is the most stable configuration. M1–M3 modes are typical of chemisorption. Upon O_2 adsorption, the oxygen species adsorbed on CuCl(1 1 1) surface mainly exists in the form of the superoxo (O_2^-).

3.3. O_2 dissociation on the CuCl(1 1 1) surface

To obtain further detailed understanding about the catalytic activity of CuCl(1 1 1) surface for O_2 dissociation, we need to determine accurate activation barrier of O_2 dissociation. So the complete LST/QST approach is chosen to search for the transition states of reactions [58], starting from reactants and products, the LST (Linear Synchronous Transit) method performs a single interpolation to a maximum energy, and the QST (Quadratic Synchronous Transit) method alternates searches for an energy maximum with constrained minimizations in order to refine the transition state to a high degree. The dissociation of O_2 on CuCl(1 1 1) surface is investigated with one molecule in every (2×2) unit cell, as a result, the initial state represents a molecular coverage of 1/4 ML, leading to a dissociated final state with an atomic coverage of 1/2 ML.

Since M1–M3 modes are the stable adsorption configurations towards the dissociation of O_2, they are naturally chosen as the initial reactants for O_2 dissociation, as described in Fig. 5, and the product P1 (two atomic O are adsorbed at two adjacent hollow sites) is employed as the final product of O_2 dissociation process, as presented in Fig. 3(c). The calculated reaction energies and relevant activation barriers of the rate-determining step for O_2 dissociation on CuCl(1 1 1) surface are collected in Table 3.

From Table 3, it can be seen that the dissociation process of O_2 on CuCl(1 1 1) surface into P1 for M1 mode is an elementary reaction,

Table 2
The calculated properties of O_2 adsorbed at different sites on CuCl(1 1 1) surface.[a]

Adsorption mode	r(O–O)/nm	$q(O_2)$	E_{ads}/kJ mol^{-1}	ν(O–O)/cm^{-1}
Top-V	0.133 (0.135)	−0.400 (−0.440)	138.9 (146.1)	1022 (970)
Bridge-V	0.135 (0.136)	−0.440 (−0.481)	146.1 (145.6)	979 (930)
Cl site-V	0.135 (0.136)	−0.440 (−0.481)	146.1 (145.6)	978 (930)
Hollow-V	0.131 (0.132)	−0.375 (−0.441)	87.9 (70.9)	1151 (1090)
Top-P	0.135 (0.136)	−0.440 (−0.481)	146.1 (145.6)	980 (931)
Bridge-P	0.133 (0.136)	−0.399 (−0.479)	138.9 (145.6)	1029 (919)
Cl site-P	0.135 (0.136)	−0.439 (−0.479)	146.1 (145.6)	980 (921)
Hollow-P	0.135 (0.136)	−0.439 (−0.477)	146.1 (145.6)	980 (924)
Free O_2	0.122			1557
O_2^- [55,56]	0.128			~1097
O_2^{2-} [55,56]	0.149			~766

[a] The values in parentheses is that of O_2 in the singlet state adsorbed at different sites on CuCl(1 1 1) surface.

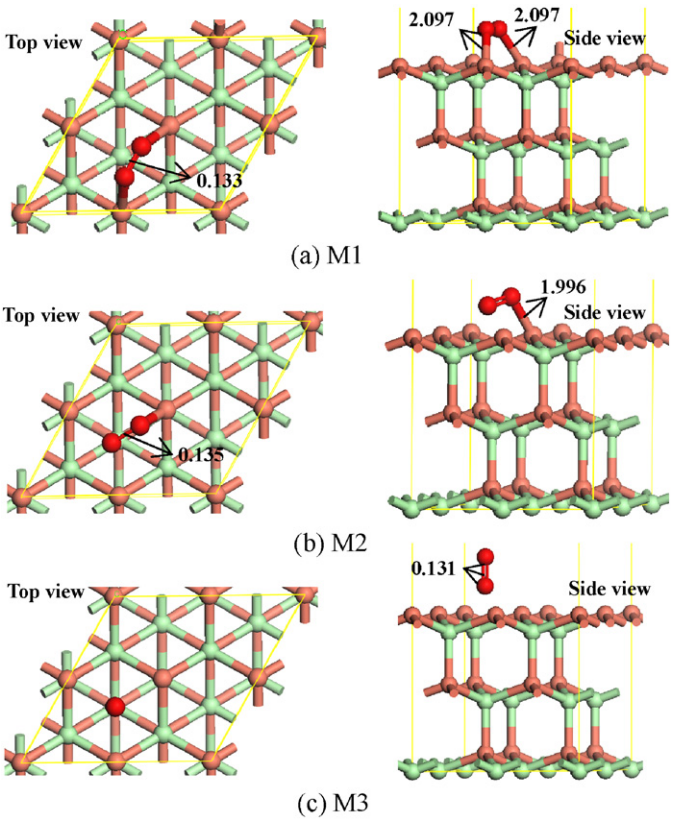

Fig. 5. The optimized equilibrium configurations of O_2 adsorbed at different sites of CuCl(1 1 1) surface. See Figs. 1 and 2 for color coding.

which needs to overcome an activation barrier by 195.2 kJ mol^{-1}, and the corresponding reaction energy is strongly endothermic by 154.1 kJ mol^{-1}. Further, for the dissociation of O_2 in M2 mode, the activation barrier is 220.1 kJ mol^{-1}, and the corresponding reaction energy is also highly endothermic by 170.5 kJ mol^{-1}. Finally, for the dissociation of O_2 in M3 mode, it consists of two elementary reactions, M3 firstly converts into an intermediate, which is similar to M2 mode, and the corresponding O–O bond length of O_2 is elongated to 0.136 nm, this elementary reaction has an activation barrier of 30.4 kJ mol^{-1} and a reaction energy of −73.8 kJ mol^{-1}. Then, the O–O bond in this intermediate further dissociates into P1, in which the activation barrier and reaction energy are 219.3 kJ mol^{-1} and 170.7 kJ mol^{-1}, respectively. Accordingly, the bond dissociation energy of free O_2 molecule obtained by experiment is 506.2 kJ mol^{-1} [43], it can be inferred that CuCl(1 1 1) surface has the effective catalytic activity for O_2 dissociation. But our kinetics results show that the dissociation of O_2 into two atomic O needs to overcome the high activation barriers, and the corresponding reaction is highly endothermic, suggesting that upon O_2 adsorption, the oxygen species adsorbed on CuCl(1 1 1) surface mainly exists in the form of molecular oxygen, which shows the characteristic of the superoxo (O_2^-) form, meanwhile, a small quantity of O_2 dissociation into atomic O for M1–M3 modes also occur, which need to overcome a large activation barrier.

Table 3
The reaction energies (ΔE) and relevant activation barriers (E_a) of the rate-determining step for O_2 dissociation on CuCl(1 1 1) surface.

Dissociation reaction	E_a/kJ mol^{-1}	ΔE/kJ mol^{-1}
M1 → P1	195.2	154.1
M2 → P1	220.1	170.5
M3 → P1	219.3	170.7

Therefore, based on our calculated results, we can think that the existent state of oxygen species on CuCl(1 1 1) surface mainly exists in the form of the superoxo (O_2^-), which plays a key role for the formation of CH_3O in DMC synthesis, and the presence of the superoxo primarily contribute to improving the catalytic activity of CuCl for CH_3O formation, which is supported by the experimental facts that the important intermediate CH_3O can be easily formed by CH_3OH decomposition in the presence of oxygen species for DMC synthesis over Cu-based catalyst [23,10,24–26]. Meanwhile, our results can provide some microscopic information for the understanding of the catalytic mechanism of DMC synthesis over CuCl catalyst from oxidative carbonylation of methanol. So in our future work, we will focus on the studies about catalytic mechanism of CH_3O formation in the presence of the superoxo.

4. Conclusions

A detailed density functional study with periodical slab calculations have been performed to illustrate the adsorption and dissociation of molecular and atomic oxygen on CuCl(1 1 1) surface. The optimized geometries, adsorption energies, vibrational frequencies and Mulliken charges show that atomic oxygen preferentially adsorbs at hollow site. Molecular O_2 lying flatly on the surface is the most advantageous adsorption configuration; the oxygen species show the characteristic of the superoxo (O_2^-). Meanwhile, the kinetics results suggest that although a small quantity of O_2 dissociation into atomic O also occurs, it needs to overcome very large activation barrier, which means that the existent state of oxygen species on CuCl(1 1 1) surface mainly exists in the form of the superoxo (O_2^-). Therefore, based on the experimental facts, our calculated results can illuminate that the presence of the superoxo mainly contributes to improving the catalytic activity of CuCl for the formation of CH_3O, which may provide some microscopic information for the understanding of the catalytic mechanism of DMC synthesis over CuCl catalyst from oxidative carbonylation of methanol.

Acknowledgement

The authors gratefully acknowledge the financial support of this study by the National Natural Science Foundation of China (20906066, 20976115 and 20976113).

References

[1] U. Romano, R. Tesel, M.M. Mauri, P. Rebora, Ind. Eng. Chem. Prod. Res. Dev. 19 (1980) 396–403.
[2] M.A. Pacheco, C.L. Marshall, Energy Fuels 11 (1997) 2–29.
[3] Y. Sato, M. Kagotani, T. Yamamoto, Y. Souma, Appl. Catal. A 185 (1999) 219–226.
[4] J.C. Hu, Y. Cao, P. Yang, J.F. Deng, K.N. Fan, J. Mol. Catal. A: Chem. 185 (2002) 1–9.
[5] V. Raab, M. Merz, J. Sundermeyer, J. Mol. Catal. A: Chem. 175 (2001) 51–63.
[6] W.L. Mo, H. Xiong, T. Li, X.C. Guo, G.X. Li, J. Mol. Catal. A: Chem. 247 (2006) 227–232.
[7] Y. Sato, M. Kagotani, Y. Souma, J. Mol. Catal. A: Chem. 151 (2000) 79–85.
[8] W.L. Mo, H.T. Liu, H. Xiong, M. Li, G.X. Li, Appl. Catal. A: Gen. 333 (2007) 172–176.
[9] Y. Cao, J.F. Hu, P. Yang, W.L. Dai, K.N. Fan, Chem. Commun. 7 (2003) 908–909.
[10] S.T. King, J. Catal. 161 (1996) 530–538.
[11] S. Csihony, L.T. Mika, G. Vlád, K. Barta, C.P. Mehnert, I.T. Horváth, Collect. Czech. Chem. Commun. 72 (2007) 1094–1106.
[12] M. Richter, M.J.G. Fait, R. Eckelt, M. Schneider, J. Radnik, D. Heidemann, R. Fricke, J. Catal. 245 (2007) 11–24.
[13] R.G. Zhang, L.X. Ling, B.J. Wang, W. Huang, Appl. Surf. Sci. 256 (2010) 6717–6722.
[14] J. Ren, S.S. Liu, Z. Li, X.L. Lu, K.C. Xie, Appl. Catal. A: Gen. 366 (2009) 93–101.
[15] J. Ren, S.S. Liu, Z. Li, K.C. Xie, Catal. Commun. 12 (2011) 357–361.
[16] J. Ren, Z. Li, S.S. Liu, Y.L. Xing, K.C. Xie, Catal. Lett. 124 (2008) 185–194.
[17] Z. Li, S.S. Liu, J. Ren, Y.Y. Niu, H.Y. Zheng, Q. Zhao, L.P. Cui, Chin. J. Catal. 31 (2010) 683–688.
[18] Z. Li, F.H. Meng, J. Ren, H.Y. Zheng, K.C. Xie, Chin. J. Catal. 29 (2008) 643–648.
[19] J. Ren, Z. Li, S.S. Liu, X.L. Lu, K.C. Xie, Kinet. Catal. 51 (2010) 250–254.
[20] M. Casarin, E. Tondello, A. Vittadini, Inorg. Chim. Acta 235 (1995) 151–158.

[21] J.Y. Lin, P. Jones, J. Guckert, E.I. Sokomon, J. Am. Chem. Soc. 113 (1991) 8312–8326.
[22] E.J. Solomon, P.M. Jones, J.A. May, Chem. Rev. 93 (1993) 2623–2644.
[23] S.T. King, Catal. Today 33 (1997) 173–182.
[24] S.A. Anderson, S. Manthata, T.W. Root, Appl. Catal. A: Gen. 280 (2005) 117–124.
[25] S.A. Anderson, T.W. Root, J. Catal. 217 (2003) 396–405.
[26] Y.H. Zhang, A.T. Bell, J. Catal. 255 (2008) 153–161.
[27] X. Wang, W.K. Chen, C.H. Lu, Appl. Surf. Sci. 254 (2008) 4421–4431.
[28] T. Yang, X.D. Wen, C.F. Huo, Y.W. Li, J.G. Wang, H.J. Jiao, J. Mol. Catal. A: Chem. 302 (2009) 129–136.
[29] P. Lukinskas, D. Fărcaşiu, Appl. Catal. A: Gen. 209 (2001) 193–205.
[30] M.Y. Sun, A.E. Nelson, J. Adjaye, J. Catal. 233 (2005) 411–421.
[31] M. Pozzo, D. Alfè, Int. J. Hydrogen Energy 34 (2009) 1922–1930.
[32] X. Wang, W.K. Chen, X.L. Xu, C.H. Lu, Chin. J. Catal. 28 (2007) 696–702.
[33] S. Kono, T. Ishii, T. Sagawa, T. Kobayasi, Phys. Rev. B 8 (1973) 795–803.
[34] D. Westphal, A. Goldmann, J. Phys. C: Solid State Phys. 15 (1982) 6661–6671.
[35] D. Westphal, A. Goldmann, Solid State Commun. 35 (1980) 441–444.
[36] W.K. Chen, X. Wang, Z.H. Chen, C.H. Lu, J.D. Zheng, Chin. J. Catal. 29 (2008) 748–752.
[37] X. Wang, W.K. Chen, B.Z. Sun, C.H. Lu, Chin. J. Inorg. Chem. 23 (2007) 807–812.
[38] X. Wang, W.K. Chen, B.Z. Sun, C.H. Lu, Chin. J. Chem. Phys. 21 (2008) 39–44.
[39] R.G. Zhang, H.Y. Liu, L.X. Ling, Z. Li, B.J. Wang, Appl. Surf. Sci. 257 (2011) 4232–4238.
[40] P. Hu, D.A. King, S. Crampin, M.H. Lee, M.C. Payne, Chem. Phys. Lett. 230 (1994) 501–506.
[41] J.P. Perdew, J.A. Chevary, S.H. Vosko, K.A. Jackson, M.R. Pederson, D.J. Singh, C. Fiolhais, Phys. Rev. B 46 (1992) 6671–6687.
[42] R.G. Zhang, B.J. Wang, L.X. Ling, H.Y. Liu, W. Huang, Appl. Surf. Sci. 257 (2010) 1175–1180.
[43] J.P. Perdew, K. Burke, M. Ernzerhof, Phys. Rev. Lett. 77 (1996) 3865–3868.
[44] J.P. Perdew, Y. Wang, Phys. Rev. B 45 (1992) 13244–13249.
[45] Y. Inada, H. Orita, J. Comput. Chem. 29 (2008) 225–232.
[46] M. Dolg, U. Wedig, H. Stoll, H. Preuss, J. Chem. Phys. 86 (1987) 866–872.
[47] A. Bergner, M. Dolg, W. Kuechle, H. Stoll, H. Preuss, Mol. Phys. 80 (1993) 1431–1441.
[48] B. Delley, J. Chem. Phys. 92 (1990) 508–517.
[49] B. Delley, J. Chem. Phys. 113 (2000) 7756–7764.
[50] D.R. Lide, Handbook of Chemistry and Physics, 82nd ed., CRC Press, Boca Raton, 2001.
[51] G. Herzberg, Molecular Spectra and Molecular Structure. II. Infrared and Raman Spectra of Polyatomic Molecules, Lancaster Press, New York, 1946, p. 365.
[52] K.H. Schulz, D.F. Cox, Phys. Rev. B 43 (1991) 1610–1621.
[53] R.G. Zhang, H.Y. Liu, H.Y. Zheng, L.X. Ling, Z. Li, B.J. Wang, Appl. Surf. Sci. 257 (2011) 4787–4794.
[54] N.C. Baenziger, S.L. Modak, C.L. Fox, J. Acta Crystallogr. C 39 (1983) 1620–1623.
[55] B.Z. Sun, W.K. Chen, X. Wang, Y. Li, C.H. Lu, Chin. J. Inorg. Chem. 24 (2008) 340–350.
[56] K. Nakamoto, Infrared and Raman Spectra of Inorganic and Coordination Compounds, 4th ed., John Wiley and Sons Press, New York, 1986.
[57] L.N. Zhang, M.F. Zhou, M.H. Chen, Q.Z. Qin, Chem. Phys. Lett. 325 (2000) 447–452.
[58] T.A. Halgren, W.N. Lipscomb, Chem. Phys. Lett. 49 (1977) 225–232.